Received: 21 June 2021 | Revised: 4 February 2022 | Accepted: 11 February 2022

DOI: 10.1002/we.2724

RESEARCH ARTICLE

WILEY

Lidar-based feedforward control design methodology for tower load alleviation in wind turbines

Irene Miquelez-Madariaga[1] | Idoia Lizarraga-Zubeldia[1] | Asier Diaz de Corcuera[2] | Jorge Elso[1]

[1]Department of Engineering, Public University of Navarre, Pamplona, Spain

[2]Siemens Gamesa Renewable Energy, Sarriguren, Spain

Correspondence
Irene Miquelez-Madariaga, Department of Engineering, Public University of Navarre, Pamplona, Spain.
Email: irene.miquelez@unavarra.es

Funding information
Siemens Gamesa Renewable Energy, Grant/Award Number: 1055/2020

Summary

Minimising tower loads is a key issue for the optimal operation and cost-effective design of wind turbines. Light detection and ranging (LIDAR) technologies enable the measurement of free wind ahead of the rotor and the addition of new feedforward controllers to the traditional control loops, improving the performance in terms of generator speed regulation and load reduction. This paper presents a design procedure based on plant inversion at a set of key frequencies. Tower base longitudinal bending moment is considered the main output of the system. Although the minimisation of tower base loads is the main objective of the design, good results are obtained in terms of generator speed regulation and pitch actuation as well. The methodology has been tested in the well-known NREL 5MW wind turbine. Results have been obtained for different LIDAR configurations in order to quantify the loss of performance due to measurement errors. In all cases, the feedforward control behaves better than the baseline case.

KEYWORDS
LIDAR, load alleviation, wind turbine

1 | INTRODUCTION

Maximum power production and load reduction are the main objectives in the design of controllers for wind turbines, as they relate to cost-effective construction and longer operation. More specifically, at above rated operation, control loops must ensure a constant generator speed and low loads on structural components such as the tower, the blades or the shaft.

Due to the poor wind information provided by traditional anemometry, control objectives are achieved with feedback loops based on the measurement of signals such as generator speed and nacelle acceleration. In recent years, light detection and ranging (LIDAR) sensors have changed this scenario, generating a great interest due to their particular measuring characteristics: they provide an undisturbed measurement of the wind before it reaches the rotor.

Owing to their promising performance and their ever improving functionalities and cost-effectivity, there exist many design proposals that include LIDAR measurements in the control loops. Although the actual benefits of using LIDAR measurements for power capture enhancement at below rated operation are not clear, load reduction and generator speed regulation objectives at above rated operation seem to profit from the inclusion of feedforward controllers.[1]

A first group of proposals is based on the inversion of the linear model. More specifically, they aim to solve the problem caused by the presence of nonminimum phase zeros in the transfer functions describing the behaviour of the system, which makes a complete model inversion impossible. These strategies range from simpler solutions that use only low frequency gains and avoid high order dynamics to more complex approximations of the inverse transfer functions such as non-causal series expansion, both for a better regulation[2–5] and for reducing mechanical loads.[6] A similar approach can be followed for non linear models.[7]

The preview information offered by LIDAR sensors opens the door to more advanced techniques based on the online calculation of optimal control actions, such as Model Predictive Control,[8–10] adaptative feedforward controllers,[11] Receding Horizon Control[12] or Preview Control.[4]

During the last years, LIDAR assisted control (LAC) has evolved towards more sophisticated solutions like robust control based on bladed mounted LIDARS.[13] Besides, LAC has been able to provide solutions to more complex scenarios, such as offshore wind turbines.[14,15]

Some authors[8] have compared simple model inversion proposals and advance methodologies such as Model Predictive Control. While the first group of proposals are easy to implement and are less computationally expensive, advanced solutions provide better multiobjective performance.[16] This fact is evidenced when realistic wind measurements are taken into account, which requires some degree of robustness in the design.[10]

The present document describes a design procedure that preserves the simplicity of the model inversion approach, while allowing a load reduction-oriented design. One of the main contributions of this work is a frequency domain analysis of the system to determine the range of frequency in which control action is most beneficial. Besides, a linear frequency domain approach to partial model inversion is proposed for the design of a feedforward controller. Lastly, the tower base load is chosen as the main output of the linear system and, thus, its reduction becomes the main objective of the feedforward controller.

The structure of the paper goes as follows. Section 2 includes a description of the simulation environment and the LIDAR simulator. The design methodology is introduced in Section 3, and simulation results are presented in Section 4. Section 5 contains the concluding remarks.

2 | SIMULATION ENVIRONMENT

The simulation environment in which the control proposal has been evaluated is based on the tools provided by NREL, namely, the preprocessor TurbSim[17] for wind field generation, the aeroelastic simulator FAST[18] and its linearising tool, and the postprocessor MLIFE.[19]

2.1 | Wind turbine

The wind turbine used in the study is the 5 MW NREL model,[20] which is an onshore, horizontal axis, three bladed turbine. The most relevant parameters of the model are presented in Table 1.

FAST allows the user to deactivate the turbine degrees of freedom both during simulation and linearisation. For this study to be as close to reality as possible, all degrees of freedom except from the rotor teeter are kept activated.

2.2 | Feedback control structure

FAST provides a MATLAB interface that allows to integrate the simulator as a block within a Simulink model. Thus, any control strategy can be easily implemented.

The complete control system comprises several control loops[21] that are activated or deactivated depending on the operation region of the wind turbine. At lower wind speeds, the main control objective is to maximise the produced power. Hence, pitch angle is kept equal to zero and

TABLE 1 Parameters for the 5 MW NREL wind turbine[20]

Parameter	Value
Rotor diameter	126 m
Hub height	90 m
Cut-in rotor speed	6.9 rpm
Rated rotor speed	12.1 rpm

generator torque is adjusted for a maximum power tracking. At higher wind speeds, when the wind turbine is operating at its rated generator speed, torque is held at its nominal value and pitch actuator is used so that power remains constant. The feedback controller consists in a PI controller and a first order lowpass filter, whose main parameters are summarised in Table 2 for different operation points. The parameters of the resulting controllers are scheduled using an estimation of the wind speed.

Transitions between these regimes are commanded by a state machine, whose input signals are pitch angle, generator speed, and generator torque. Additionally, as shown in Figure 1, the first fore-aft vibrational mode of the tower and the drive train torsional vibration are reduced with the strategies proposed in Bossanyi.[21]

2.3 | LIDAR simulator

In order to include the feedforward controller in the simulation model, a wind signal is required as its input. With the aim of obtaining the best performance of the design, the Rotor Effective Wind Speed[22] (REWS) signal is used in a first set of simulations. The REWS is defined theoretically as

TABLE 2 Baseline feedback control parameters

Wind (ms^{-1})	Phase margin (°)	Cross-over freq. (Hz)	Pole (Hz)
12	60	0.05	0.45
16	50	0.08	0.6
20	55	0.12	0.5
24	50	0.13	0.5

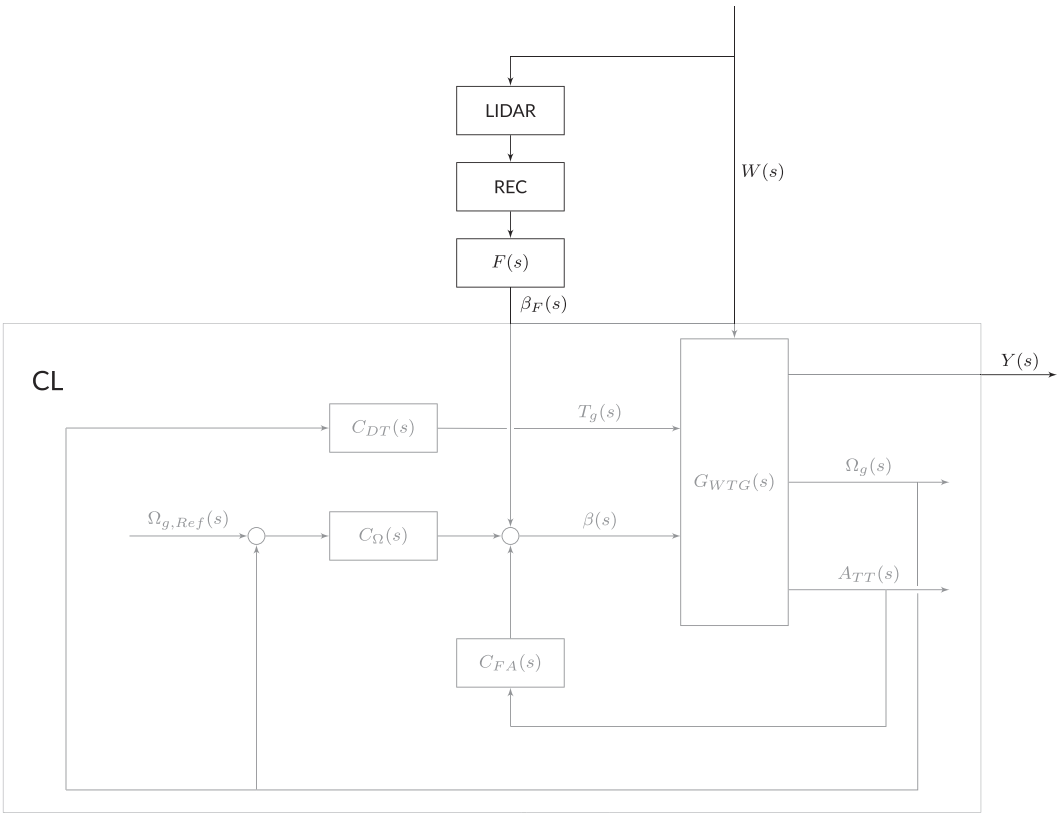

FIGURE 1 Diagram of the control loops. $C_\Omega(s)$ is designed to ensure a correct generator speed regulation, $C_{DT}(s)$ reduces the torsional loads in the drive train and $C_{FA}(s)$ is designed to reduce the first fore-aft vibrational mode of the tower. Block $F(s)$ corresponds to the feedforward controller and REC to the reconstruction stage described in Section 2.3. All the blocks enclosed in the gray area form the closed loop linear system used for the design of the feedforward controller

$$v_e = \sqrt[3]{\frac{\int_0^{2\pi}\int_0^R v_u^3(r,\varphi)\frac{\partial c_P}{\partial r}drd\varphi}{\int_0^{2\pi}\int_0^R \frac{\partial c_P}{\partial r}drd\varphi}}, \quad (1)$$

where v_u is the wind speed in the direction perpendicular to the rotor, r and φ are the polar coordinates in the rotor plane, and c_P is the power coefficient of the wind turbine.

In practice, REWS is calculated from the wind field generated by TurbSim, with a grid of 31 × 31 points and a sampling frequency of 50 Hz, as the average in the rotor plane of the wind speed perpendicular to it. The calculation is performed offline and the signal is introduced into Simulink for each simulation.

Additionally, a LIDAR simulator[23] has been included into the Simulink control structure, which uses the time series of three-dimensional wind velocity vectors at the rotor plane generated by TurbSim for obtaining a realistic LIDAR measurement. The simulator introduces the sources of error that usually appear in nacelle-mounted LIDARs, such as the information loss due to spatial and temporal sampling and blade crossing, the effect of nacelle movement, the spatial averaging of the measurement along the volume of the beam and the projection of wind speed into the beam direction.

The simulator has a variable configuration in terms of the number and the geometry of the beams. For an evaluation of the measurement error effect in the simulation results, two different configurations have been used. The first one (see Figure 2A) measures 4 points 88 m ahead of the rotor plane with a half cone angle of 28°. The second one (see Figure 2B) measures 40 points 88 m ahead of the rotor with 10 different opening angles between 3° and 28°.

Besides the simulation of the sensor, a reconstruction stage is included in the model. Its objective is to transform the information given by the sensor into a signal resembling the REWS as closely as possible. The reconstruction process consist of several steps, common to any of the LIDAR configurations:

- lost samples due to the blades crossing the beams trajectory are given the previous valid value,
- information given by the different beams is averaged,
- the resulting beam signal is filtered to remove unnecessary information at higher frequencies,using a second order filter with a cutoff frequency

$$\omega_{cutoff} = 0.7 \cdot v_{mean}, \quad (2)$$

as described by,[3] where v_{mean} is the mean windspeed at each simulation, computed offline,

- the signal is synchronised with the actual wind field by assuming Taylor's frozen turbulence hypothesis,[24] with the delay depending on the mean wind speed of each simulation.

2.4 | Baseline feedforward controller

A nonlinear feedforward controller,[3] frequently used in the bibliography as reference feedforward controller, has been implemented and compared against the controller proposed in this work. More specifically, the baseline feedforward controller aims to reduce the standard deviation of

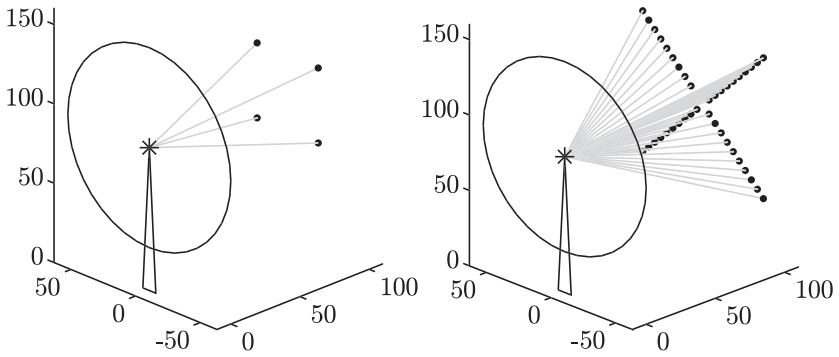

FIGURE 2 Distribution of the beams in the two implemented LIDAR simulators with 4(a) and 40(b) beams. Wind turbine dimensions are gathered in Table 1

the generator speed and consists in a lookup table made of the steady state pitch values obtained from a reduced system (Figure 3). This controller works at above rated wind speeds and, given a perfect wind preview, it compensates perfectly the effect of wind on the generator speed and helps reducing loads in the tower.

2.5 | Turbulent winds

The turbulent wind fields used in simulation are generated with the preprocessor TurbSim. For a complete evaluation of the performance of the feedforward controller, wind speeds between 13 and 25 m/s every 2 m/s have been used, with a time step of 0.02 s and a turbulence intensities of 5 and 15%. Two different seeds have been used for each combination of mean speed and turbulence intensity, making a total of 28 simulations, with a length of 550 s each.

3 | CONTROLLER DESIGN

The developed controller is based on the inversion of the linear model, and thus, the first step in the design is to obtain the model of the 5 MW wind turbine by using FAST linearisation tool, represented as $G_{WTG}(s)$ in Figure 1. Then, the controllers $C_{\Omega}(s)$, $C_{FA}(s)$ and $C_{DT}(s)$ defined in Figure 1, which are also linear, are added to form the closed loop system, represented in Figure 1 as the grey block CL. The resulting system has two inputs, the wind ($W(s)$) and the feedforward control pitch action ($\beta_F(s)$), whose effect on a generic output $Y(s)$ is represented by a pair of transfer functions, $D_{CL}(s)$ and $P_{CL}(s)$, respectively.

Following this structure, if a pitch feedforward controller $FF(s)$ is added to the baseline control and assuming the LIDAR provides perfect preview, the effect of the wind $W(s)$ in a generic output $Y(s)$ is given by

$$Y(s) = (D_{CL}(s) + F(s) \cdot P_{CL}(s)) \cdot W(s), \tag{3}$$

as shown in Figure 4. $F(s)$ should be adjusted to completely eliminate the effect of $W(s)$ on $Y(s)$. Thus, by making

$$\frac{Y(s)}{W(s)} = 0, \tag{4}$$

the feedforward controller transfer function should be calculated as

$$F(s) = -\frac{D_{CL}(s)}{P_{CL}(s)}. \tag{5}$$

In other words, the feedforward controller is able to cancel out all effect from the wind to the output, if it provides an inversely phased signal with the same amplitude as the wind does.

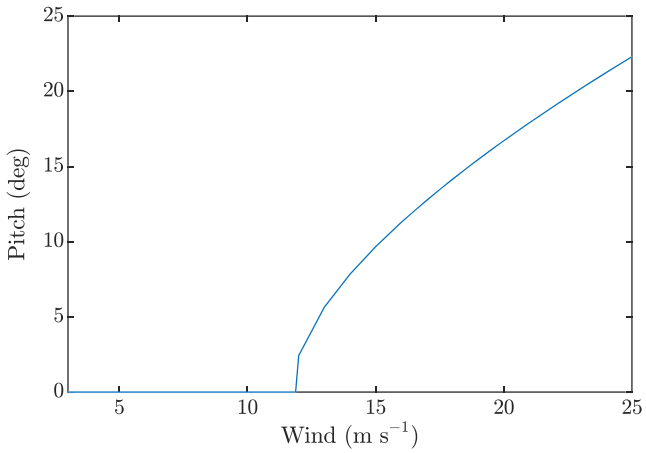

FIGURE 3 Static pitch curve of the 5MW wind turbine [Colour figure can be viewed at wileyonlinelibrary.com]

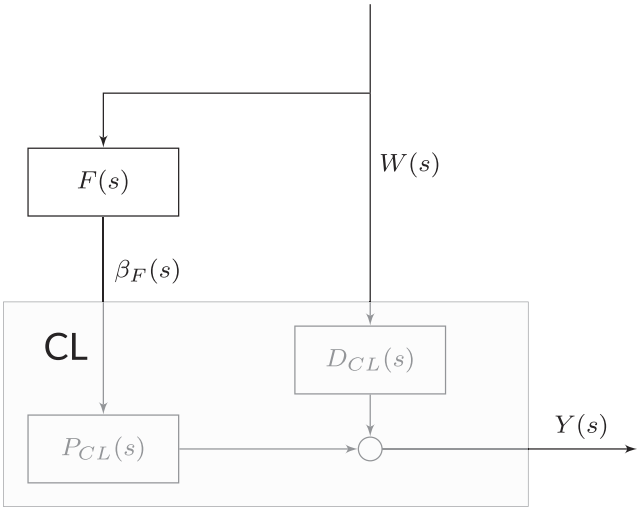

FIGURE 4 Diagram of the closed-loop system with a feedforward controller

Due to the presence of non minimum phase zeros in the system, it is not possible to obtain the feedforward controller as given by Equation (5), as it would lead to an unstable controller. As previously mentioned, several of the proposals given by the literature solve this problem by approximating the unstable poles of the controller given by Equation (5). Besides, they use the generator speed as output, thus setting speed regulation as the most important control objective.

The present work aims to keep the straightforward approach of model inversion but introducing two substantial changes. The first one consists in choosing the tower base longitudinal bending moment as output signal of the transfer functions used in the design. Consequently, load reduction becomes the main control objective. Secondly, the controller is designed in the frequency domain by using the information provided by the Bode diagram of the closed-loop the system. To do so, the design condition expressed by the complex equation (5) can be rewritten as a magnitude condition

$$|F(i\omega)| = \frac{|D_{CL}(i\omega)|}{|P_{CL}(i\omega)|}, \tag{6}$$

and a phase condition

$$\varphi(F(i\omega)) = \varphi(D_{CL}(i\omega)) - \varphi(P_{CL}(i\omega)) - 180^{\circ}, \tag{7}$$

where φ is the phase of a given transfer function at frequency ω and the 180° term in the phase condition corresponds to the negative sign in Equation (5).

As a complete model inversion is not possible, there exists no stable transfer function fulfiling conditions (6) and (7) at every frequency. However, it is easy to meet them at a single frequency ω_0, which must be chosen to reach the control objective—tower base load reduction—in the best possible way.

A first condition on ω_0 is that it must be located in the frequency range in which the effective wind appears, as the spectrum of the signal that enters the controller will determine its output. According to the amplitude spectrum of the effective wind, shown in Figure 5, an upper limit to ω_0 is at 2 rad/s. A second relevant factor is the behaviour of the system prior to adding the feedforward controller. In other words, loads should be reduced in the frequencies in which they are more damaging to the wind turbine.

Conventionally, the effect of loads in terms of fatigue is expressed by the damage equivalent load (DEL). As the linear system in the form of the transfer function $D_{CL}(s)$ only provides a frequency domain relation between the wind and the load signals, it is necessary to establish a frequency domain relation between the load signal and the damage equivalent load. Firstly, the load signal is decomposed into its discrete Fourier transform, and thus, can be written as

$$My_{TB} = \left(\sum_{j=0}^{j=N} |My_{TBj}| cos(\omega_j t + \phi_j) \right). \tag{8}$$

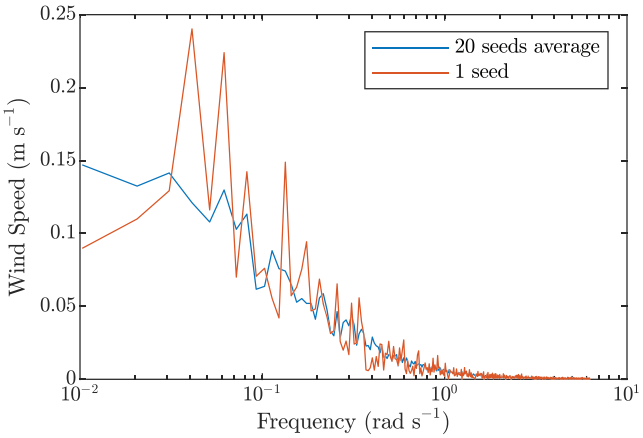

FIGURE 5 Amplitude spectrum of the rotor effective wind speed for a wind field of mean speed 15 m/s and a turbulence intensity of 15% [Colour figure can be viewed at wileyonlinelibrary.com]

With this in mind, it is possible to assemble a load signal made up of the components of My_{TB} up to a certain frequency ω_j and find the damage equivalent load they produce as

$$DEL(\omega_i) = DEL\left(\sum_{j=0}^{j=i} |My_{TBj}| cos(\omega_j t + \phi_j)\right). \tag{9}$$

Repeating the process for ω_{i+1} an dividing the difference in loads by the difference in frequencies,

$$\Delta DEL(\omega_i) = \frac{DEL(\omega_i) - DEL(\omega_{i-1})}{\Delta\omega} \tag{10}$$

we obtain an estimation of the load accumulated in the range ω_i to ω_{i+1}.

This way, it is possible to plot the contribution of each frequency to the overall damage equivalent load, as in Figure 6, which shows that the effect of the wind on the damage equivalent load stops being relevant at between 1 and 2 rad/s. Although the peak appearing at 3.8 rad/s contributes significantly to the fatigue damage as well, it is not possible to reduce it with a collective pitch action. As done for the effective wind speed in Figure 5, the average $DEL(\omega)$ for 20 wind seeds is used to avoid dependency of the results with a particular wind seed. As a consequence, a much smoother curve is obtained.

Taking these two factors into account, the range of frequencies for which load reduction should be pursued goes from 0.3 to 1.5 rad/s, which is precisely the range of greatest wind-to-load amplification. Clearly, conditions (6) and (7) for total attenuation cannot be met by any controller for the whole range. However, a design focused on a single frequency can be achieved by the simple lead network

$$F(s) = k \cdot \frac{1 + T \cdot a \cdot s}{1 + T \cdot s}, \tag{11}$$

whose parameters a, T, k are tuned to produce the gain and phase shift demanded by (6) and (7) at a central frequency ω_0.

In this case, ω_0 is chosen as the one at which $|D_{CL}(s)|$ peaks, as it lies in the chosen frequency range. Besides, as the changes in the slope of $P_{CL}(s)$ and $D_{CL}(s)$ at both sides of ω_0 are smooth and have the same sign, both in magnitude and phase (Figure 7), Equations (6) and (7) will almost be matched for a wide range of frequencies around ω_0. This translates into a perfect cancellation of the load at frequency ω_0 and a significant reduction at the nearby frequencies, including the range of interest, as shown in Figure 8.

The design procedure is repeated for four operation points at wind speeds between 13 m/s and 25 m/s. Then, as done for the feedback controllers, the feedforward pitch action is obtained by scheduling the four controllers using the estimation of the wind speed. In this case, instead of using scheduling of each of the parameters of the controllers, an output blending approach is used, similar to the one explained in.[25]

The result of the design process for the linear system at 13 m/s can be observed in Figure 7, where $D_{CL}(s)$ and $P_{CL}(s)F(s)$ show the same gain and a phase difference of 180° at ω_0. As a result, the overall system $D_{CL}(s) + P_{CL}(s)F(s)$ shows a downwards peak at frequency ω_0 (Figure 8).

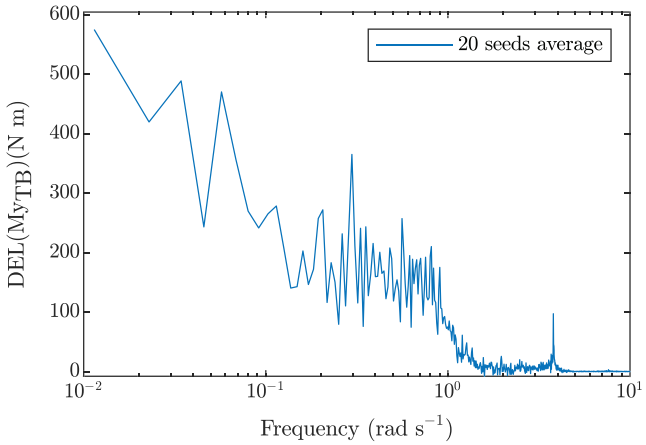

FIGURE 6 Damage equivalent load of the tower base bending moment (Equation 10) for the baseline control case in terms of the wind frequency distribution [Colour figure can be viewed at wileyonlinelibrary.com]

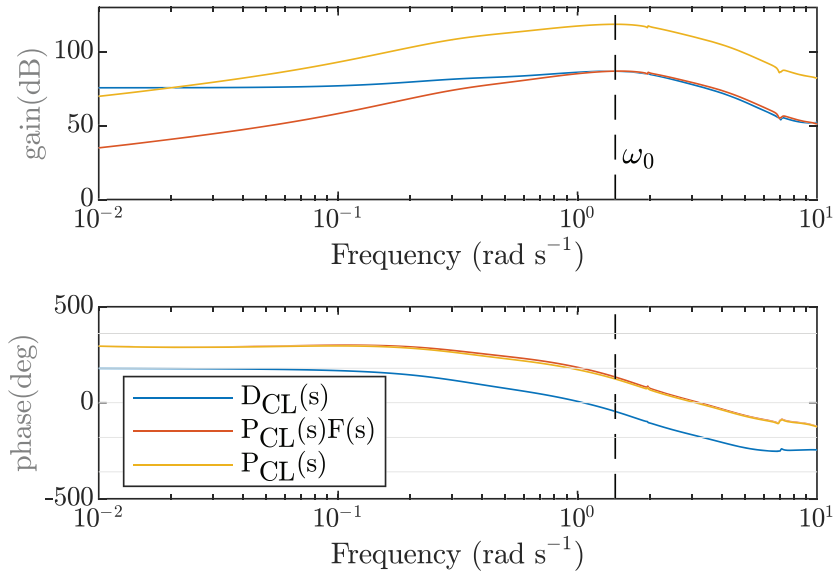

FIGURE 7 Bode diagram used for the design of the feedforward. Both for $D_{CL}(s)$ and $P_{CL}(s)F(s)$ the input signal is wind and the output signal is the tower base load. $P_{CL}(s)$ represents the effect of the feedforward pitch contribution on the tower base load [Colour figure can be viewed at wileyonlinelibrary.com]

As already mentioned, even though the main objective is to reduce the loads at the tower base, it is necessary to ensure that including the feedforward action provides a reasonable response in the other outputs. For this reason, the Bode diagram of the new linear system is compared with the baseline system, as represented in Figure 9. There, it is possible to see how, at frequencies where the effective wind appears, the magnitude of the four Bode plots is lower and, consequently, so is the effect of wind on the different outputs. In other words, adding the feedforward should provide a better generator speed regulation, a lower pitch activity and less loads in the shaft and the blades.

4 | SIMULATION RESULTS

In this section, simulation results corresponding to production winds with mean speeds ranging from 13 to 25 m/s and turbulent intensities of 5 and 15% are presented and analysed. The simulated model consists of the non linear FAST simulator, the linear feedback control scheme described in Section 2 and the feedforward control.

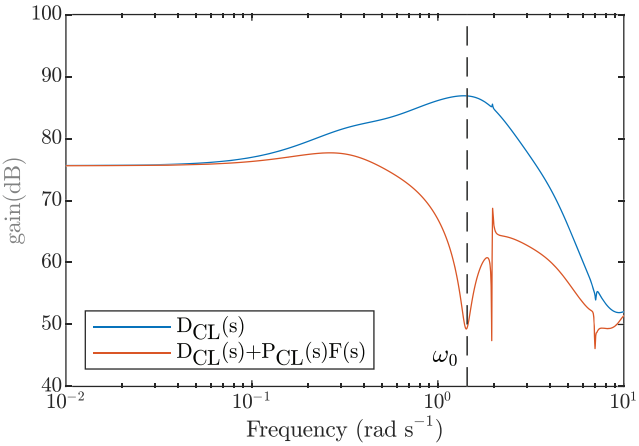

FIGURE 8 Comparison between the frequency response of the baseline control, the initial design and the final design with wind as input and tower base load as output [Colour figure can be viewed at wileyonlinelibrary.com]

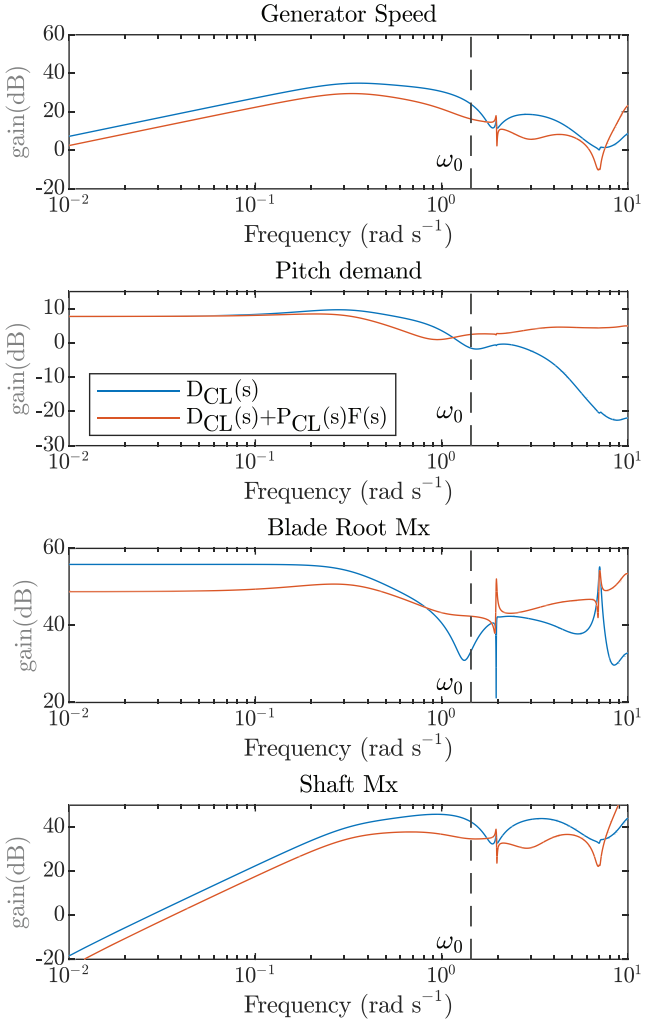

FIGURE 9 Comparison of the frequency response of the baseline control and the final design for different outputs [Colour figure can be viewed at wileyonlinelibrary.com]

Firstly, a frequency analysis of the signals obtained in simulations has been made, that confirms the validity of the linear approximation. Then, the performance of the feedforward has been assessed using conventional indicators and comparing them to the results provided by the baseline controllers.

4.1 | Relation between the linear model and the simulation results

The design methodology is based on the idea that linear models provide a good representation of the nonlinear system. To verify this assumption, the difference between simulation outputs with and without feedforward control is compared with the load reduction predicted by the bode diagrams.

Thus the discrete Fourier transform (DFT) of the tower base bending moment is calculated for the cases with feedforward controller off and on. The simulations are obtained for a wind of mean speed of 15 m/s and a turbulence intensity of 15%; 20 seeds have been simulated for each case, so that the DFTs can be averaged and the result is smoother. A linear approximation of the attenuation is obtained by multiplying the DFT of the baseline control by the load attenuation calculated as quotient of the amplitudes of the bode diagram as given by

$$My_{TB,Lin}(\omega) = \frac{|D_{CL}(\omega) + F(\omega)P_{CL}(\omega)|}{|D_{CL}(\omega)|} My_{TB,BL}(\omega). \tag{12}$$

The three signals are represented in Figure 10, where it is possible to see how the load signal obtained from the simulation of the feedforward and the linear approximation obtained from the simulation of the baseline system bear a great resemblance in the lower frequencies and become different in the higher ones. This difference at the higher frequencies can be caused by several phenomena such as the operation of the wind turbine at different points due to changes in wind or the fact that the effective wind speed does not fully represent the effect of the wind in the loads.

4.2 | Fatigue and statistical results

The quantitative assessment of the effect of the feedforward for the different control objectives is performed with the data provided by NREL's postprocessor MLIFE. More specifically, fatigue is evaluated by means of the damage equivalent load, generator speed regulation and pitch actuation are considered in terms of their standard deviations and energy production is assessed by the mean power production. The feedforward controller is first compared with the feedback only case and then to the baseline feedforward control (Figures 12 and 13).

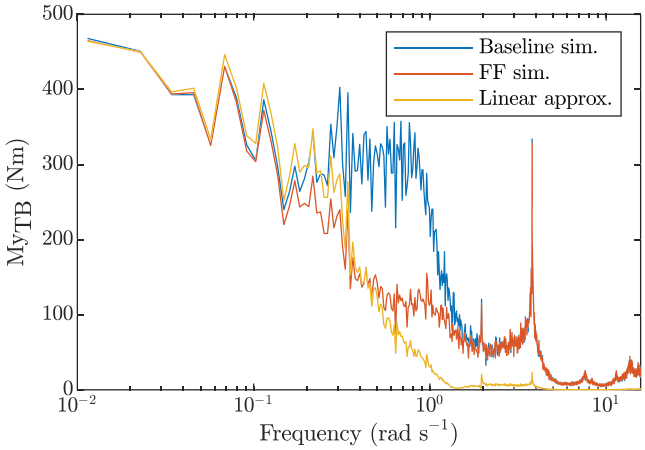

FIGURE 10 Amplitude spectra of the tower base bending moment obtained by the simulation of the baseline system (20 seeds average), simulation of the system with feedforward (20 seeds average) and linear approximation of the effect of the feedforward by applying the attenuation predicted from the Bode diagrams to the results of the baseline simulation for a wind with mean speed 15 m/s and turbulence intensity of 15% [Colour figure can be viewed at wileyonlinelibrary.com]

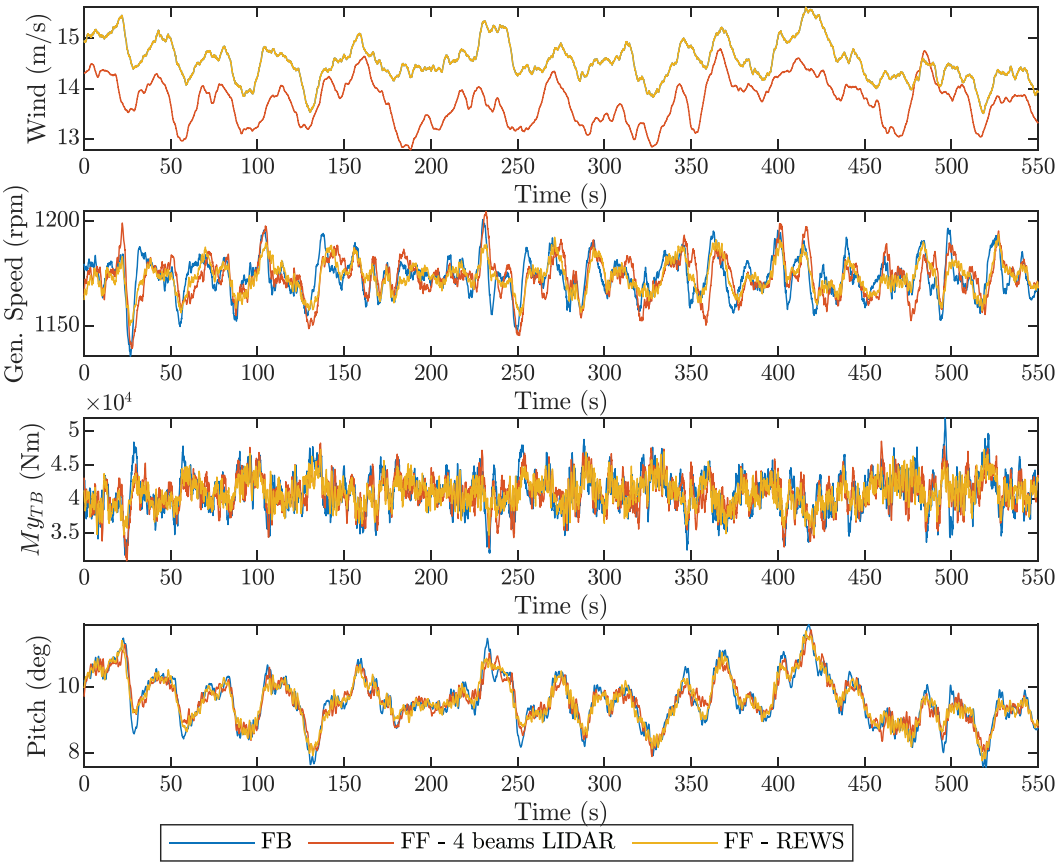

FIGURE 11 Simulation output time series with the baseline control, the feedforward fed by a 4 beam LIDAR simulator and the feedforward fed with the REWS [Colour figure can be viewed at wileyonlinelibrary.com]

Figure 11 shows some of the simulation outcomes used by MLIFE for the calculation of fatigue and statistical results. For the same wind field, it is clear how oscillations in generator speed, tower base bending moment and pitch are reduced when using feedforward compared with the feedback control, even with a realistic LIDAR simulator. This translates into a better fulfilment of the regulation objective, smaller fatigue loads and lower pitch duty.

Figures 12 and 13 represent the overall results of the simulation sorted by turbulence intensity. As MLife provides the statistical and fatigue results for each simulation, the general picture has been obtained by averaging them using a Weibull distribution with a shape factor of 2.2 and a scale factor of 11.29.

The greatest benefits in any of the control objectives are obtained when the ideal rotor effective wind speed signal is used as input for the feedforward. In that case, tower base load is reduced by 29.66% and by 26.68% with respect to the feedback only control for the different turbulence intensities.

Additionally, loads at the shaft are reduced by 10% and loads at the blade root are reduced by 5.84% and by 13.16%. Generator speed standard deviation is substantially reduced by 33.9%, almost by 60% less than the baseline control at the higher wind speeds. Similarly, at above rated operation, pitch activity remains between by 10% smaller that the baseline control at above rate wind speeds.

The improvements obtained from the feedforward are reduced when using realistic LIDAR simulators, as they introduce an error in the reconstructed wind signal. When the error increases, for example due to a reduced number of beams, results get worse. More precisely, a 40 beam LIDAR reduces the tower base load between by 14.3% and by 11.6%, while for a 4 beam LIDAR load reduction remains between by 10.9% and by 8.75%.

Power production remains similar in all cases, with independence of the feedforward configuration and the wind turbulence intensity.

When compared with the feedforward baseline control (Figures 12 and 13), the trade off between control objectives becomes clear. The baseline feedforward controller excels in its intended objective—regulation of the generator speed—but it provides a worse performance at the reduction of tower base loads. Conversely, the proposed controller provides an inferior performance in generator speed regulation, although it still improves the feedback only case, but is better at reducing tower base loads.

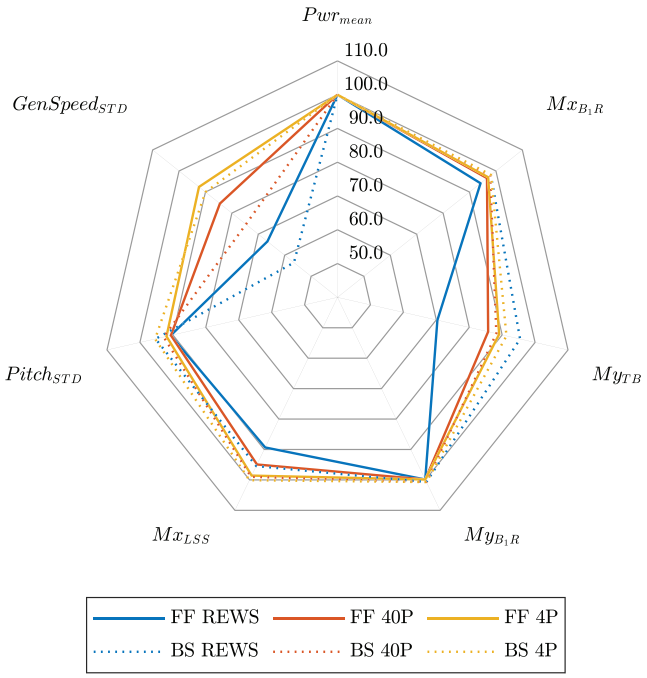

FIGURE 12 Summary of the fatigue and statistical results obtained in simulation for different LIDAR configurations and a 5% turbulence intensity, expressed with respect to the baseline feedback control results. BS corresponds to the baseline feedforward controller (static pitch curve) and FF corresponds to the load-oriented, frequency domain controller. The results correspond to the mean produced power (Pwr_{mean}), the DEL for the blade root moment in direction x ($Mx_{B_1,R}$) and y ($My_{B_1,R}$), the tower base bending moment (My_{TB}) and the moment in the shaft in direction x (Mx_{LSS}), the standard deviation of the pitch signal ($Pitch_{STD}$), and the standard deviation in the generator speed ($GenSpeed_{STD}$) [Colour figure can be viewed at wileyonlinelibrary.com]

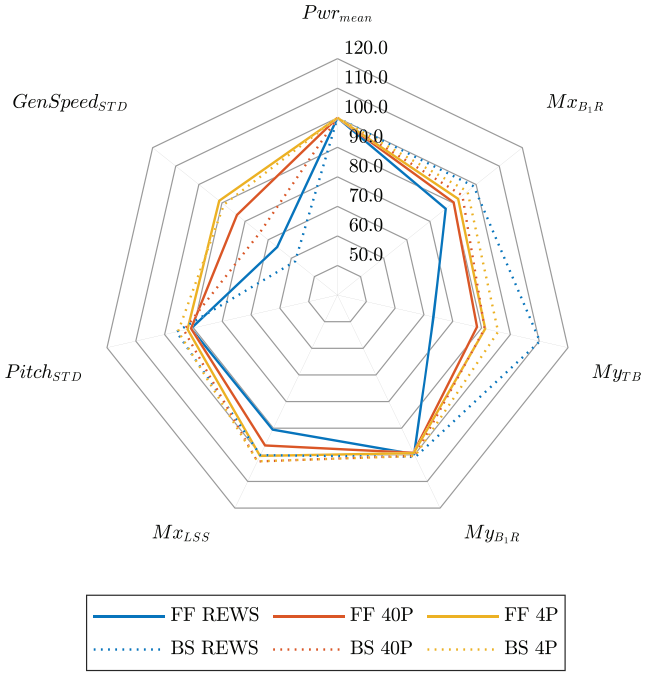

FIGURE 13 Summary of the fatigue and statistical results obtained in simulation for different LIDAR configurations and a 15% turbulence intensity, expressed with respect to the baseline feedback control results. BS corresponds to the baseline feedforward controller (static pitch curve) and FF corresponds to the load-oriented, frequency domain controller. The results correspond to the mean produced power (Pwr_{mean}), the DEL for the blade root moment in direction x ($Mx_{B_1,R}$) and y ($My_{B_1,R}$), the tower base bending moment (My_{TB}) and the moment in the shaft in direction x (Mx_{LSS}), the standard deviation of the pitch signal ($Pitch_{STD}$), and the standard deviation in the generator speed ($GenSpeed_{STD}$) [Colour figure can be viewed at wileyonlinelibrary.com]

5 | CONCLUSIONS AND FUTURE WORK

The feedforward controller design procedure presented in this paper has proven to be easy to apply for the used linear model. Besides, for the nonlinear 5 MW wind turbine, simulation results are really promising, in particular for tower load reduction, even with the loss in performance due to the use of realistic LIDAR measurements.

However, the limited structure of the controller (one zero and one pole) and the fact that the sensor measuring error has not been taken into account in the design suggest that the obtained results can be improved with more sophisticated methodologies, that could include a simultaneous design of feedback and feedforward controllers. Besides, as load reduction is clearly compatible with a better generator speed regulator, a multiobjective control problem could be studied. Lastly, simulation results suggest that an specific design for the rated wind speeds could significantly improve the overall performance.

ACKNOWLEDGEMENT

The authors gratefully appreciate the support given by Siemens Gamesa Renewable Energy through the predoctoral research contract no. 1055/2020.

PEER REVIEW

The peer review history for this article is available at https://publons.com/publon/10.1002/we.2724.

ORCID

Irene Miquelez-Madariaga https://orcid.org/0000-0001-6467-2154

REFERENCES

1. Schlipf D, Kapp S, Anger J, Bischoff O, Hofsäß M, Rettenmeier A, Kühn M. Prospects of optimization of energy production by LIDAR assisted control of wind turbines. European Wind Energy Association; 2011.
2. Schlipf D, Bossanyi E, Carcangiu CE, Fischer T, Maul T, Rossetti M. LIDAR assisted collective pitch control. *Technical Report*, UPWIND Deliverable D513; 2011.
3. Schlipf D. LIDAR-assisted control concepts for wind turbines. *PhD Thesis*: University of Stuttgart, Stuttgart, Germany; 2016.
4. Dunne F, Pao L, Wright A, Jonkman B, Kelley N, Simley E. Adding feedforward blade pitch control for load mitigation in wind turbines: Non-causal series expansion, preview control, and optimized fir filter methods. In: 49th AIAA Aerospace Sciences Meeting including the New Horizons Forum and Aerospace Exposition; 2011. doi:10.2514/6.2011-819
5. Dunne F, Pao L, Wright A, Jonkman B, Kelley N. Combining standard feedback controllers with feedforward blade pitch control for load mitigation in wind turbines. In: 48th AIAA Aerospace Sciences Meeting including the New Horizons Forum and Aerospace Exposition; 2010.
6. Bao J, Yue H, Leithead WE, Wang J-Q. Feedforward control for wind turbine load reduction with pseudo-LIDAR measurement. *Int J Autom Comput*. 2018;15(2):142-155.
7. Reiner MJ, Zimmer D. Nonlinear dynamic inversion control for wind turbine load mitigation based on wind speed measurement. In: Proceedings of the 11th International Modelica Conference, Versailles, France, September 21-23, 2015 Linköping University Electronic Press; 2015.
8. Schlipf D, Pao LY, Cheng PW. Comparison of feedforward and model predictive control of wind turbines using LIDAR. In: 2012 IEEE 51st IEEE Conference on Decision and Control (CDC) IEEE; 2012:3050-3055.
9. Schlipf D, Schlipf DJ, Kühn M. Nonlinear model predictive control of wind turbines using LIDAR. *Wind Energy*. 2013;16(7):1107-1129.
10. Barcena R, Acosta T, Etxebarria A, Kortabarria I. LIDAR-assisted wind turbine structural load reduction by linear single model predictive control. *IEEE Access*. 2020;8:146548-146559.
11. Wang N, Johnson KE, Wright AD. LIDAR-based FX-RLS feedforward control for wind turbine load mitigation. In: Proceedings of the 2011 American Control Conference IEEE; 2011:1910-1915.
12. Soltani M, Wisniewski R, Brath P, Boyd S. Load reduction of wind turbines using receding horizon control. In: 2011 IEEE International Conference on Control Applications (CCA) IEEE; 2011:852-857.
13. Ungurán R, Petrović V, Boersma S, van Wingerden J-W, Pao LY, Kühn M. Feedback-feedforward individual pitch control design for wind turbines with uncertain measurements. In: 2019 American Control Conference (ACC) IEEE; 2019:4151-4158.
14. Yamaguchi A, Yousefi I, Ishihara T. Reduction in the fluctuating load on wind turbines by using a combined nacelle acceleration feedback and LIDAR-based feedforward control. *Energies*. 2020;13(17):4558.
15. Schlipf D, Lemmer F, Raach S. Multi-Variable Feedforward Control for Floating Wind Turbines Using LIDAR. In: International Ocean and Polar Engineering Conference, Vol. All Days; 2020. ISOPE-I-20-1174.
16. Dunne F, Pao LY. Optimal blade pitch control with realistic preview wind measurements. *Wind Energy*. 2016;19(12):2153-2169.
17. Jonkman BJ, Buhl Jr ML. Turbsim user's guide, Golden, CO (United States), National Renewable Energy Lab.(NREL); 2006.
18. Jonkman JM, Buhl ML. Fast manual user's guide NREL. report no. nrel/el-500–38230, Golden, CO (United States), National Renewable Energy Lab. (NREL); 2005.
19. Hayman GJ, Buhl MJ. Mlife user's guide for version 1.00. 00. Oak Ridge, TN, 37831–0062; 2012.
20. Jonkman J, Butterfield S, Musial W, Scott G. Definition of a 5-MW reference wind turbine for offshore system development, Golden, CO (United States), National Renewable Energy Lab.(NREL); 2009.
21. Bossanyi EA. The design of closed loop controllers for wind turbines. *Wind Energy: An Int J Progr Appl Wind Power Convers Technol*. 2000;3(3):149-163.

22. Soltani MN, Knudsen T, Svenstrup M, et al. Estimation of rotor effective wind speed: a comparison. *IEEE Trans Control Syst Technol*. 2013;21(4):1155-1167.
23. Schlipf D, Trujillo JJ, Basterra V, Kühn M. Development of a wind turbine LIDAR simulator. Proc EWEC; 2009.
24. Schlipf D, Trabucchi D, Bischoff O, et al. Testing of frozen turbulence hypothesis for wind turbine applications with a scanning LIDAR system. In: 15th International Symposium for the Advancement of Boundary Layer Remote Sensing ISARS; 2010.
25. Aouf N, Bates DG, Postlethwaite I, Boulet B. Scheduling schemes for an integrated flight and propulsion control system. *Control Eng Pract*. 2002;10(7):685-696.

AUTHOR BIOGRAPHIES

Irene Miquelez Madariaga, MSc, received her BSc and MSc degrees in Industrial Engineering from the Public University of Navarre (UPNA) in 2016 and 2018. She is currently a PhD candidate in the Dynamic Systems and Control research group in UPNA. Her work focuses on LIDAR assisted control of wind turbines.

Idoia Lizarraga Zubeldia, MSc, received her BSc and MSc degrees in the Public University of Navarre in 2017 and 2019. She joined the Dynamic Systems and Control research group in UPNA in 2019 as a project collaborator. Her research is robust control of wind turbines.

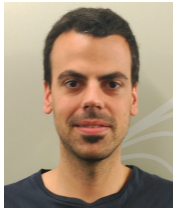

Asier Díaz de Corcuera, PhD, is a Wind Turbine Control Expert Engineer at Siemens Gamesa Renewable Energy. Previously, he received his PhD degree from University of Mondragon in 2013, while he was working in IK4-Ikerlan Research Center in wind turbine control developments (2008?2015). Thesis Dissertation was titled "Design of Robust Controllers for Load Reduction in Wind Turbines." He finished his MSc in Control Engineering and Power Electronics in University of Basque Country (UPV) in 2007.

Jorge Elso Torralba, PhD, graduated from Industrial Engineering at the Public University of Navarre in 2005 and obtained a PhD in Engineering from the same university in 2012. In 2012 and 2013, he joined the Intelligent Systems and Energy research group of the University of the Basque Country. Since 2014, he is an Assistant Professor at the Public University of Navarre. His research focuses on robust control and its application on multivariable, non-linear and distributed parameter systems. His main contributions are framed in the theory of quantitative feedback or QFT, with applications on real systems such as welding processes or wind turbines.

How to cite this article: Miquelez-Madariaga I, Lizarraga-Zubeldia I, Diaz de Corcuera A, Elso J. Lidar-based feedforward control design methodology for tower load alleviation in wind turbines. *Wind Energy*. 2022;25(7):1238-1251. doi:10.1002/we.2724